Dimorphic Intra- and Intermolecular Aryl Motifs in Symmetrical Hexafaceted Molecules $(Ar_nX)_3Y\text{-}Z\text{-}Y(XAr_n)_3$

Marcia Scudder and Ian Dance*[a]

Abstract: A variety of crystals containing molecules formulated generally as $(Ar_nX)_3Y\text{-}Z\text{-}Y(XAr_n)_3$ with exact or pseudo S_6 symmetry have been analysed for the presence of intra- and intermolecular multiple aryl embraces composed of offset-face-to-face (OFF) and edge-to-face (EF) local motifs. Ar is phenyl or substituted phenyl; $n = 1$, 2 or 3; the linkage Z is linear diatomic, linear monatomic, absent (Y−Y bond), or void (Y atoms unconnected). Representative molecular systems analysed are $(PhCH_2)_3Si\text{-}O\text{-}Si(CH_2Ph)_3$, $(PhCH_2)_3Sn\text{-}Sn(CH_2Ph)_3$, $(4\text{-}Me\text{-}C_6H_4CH_2)_3Ge\text{-}O\text{-}Ge(CH_2C_6H_4\text{-}4\text{-}Me)_3$, $[(PhS)_3Fe\text{-}O\text{-}Fe(SPh)_3]^-$, $[(PhCH_2)_3P\text{-}Cu\text{-}P(CH_2Ph)_3]^+$ and $[(Ph_3P)_3Ag\text{-}CN\text{-}Ag(PPh_3)_3]^+$. One characteristic intramolecular motif is a sixfold phenyl embrace (6PE) in which aryl groups fold back to the central domain of the molecule forming a rhombohedral box maintained by $(EF)_6$. When the aryl groups are in *exo* positions there is an $(EF)_3$ motif, like a tractor wheel, at each end of the molecule: $[(Ph_2N)_3Ti\text{-}O\text{-}Ti(NPh_2)_3]$ possesses both intramolecular motifs as $(EF)_3\text{-}(EF)_6\text{-}(EF)_3$. The molecules in this set are hexafaceted, and the crystal packing is generally based on intermolecular EF or OFF motifs with these faces, either from the central $(EF)_6$ set or the end $(EF)_3-(EF)_3$ sets. Three types of subtle crystal packing isomerism occur: 1) the faces of the rhombohedral boxlike molecules slide over each other with variation of the intermolecular motifs, forming dimorphic crystals in space groups $R\bar{3}$ or $P\bar{1}$; 2) the faces of the tractor wheels $(EF)_3$ slide over each other or 3) very similar molecules crystallise with the rhombohedral box or tractor wheel structures. In general the molecules considered are shape auspicious rather than shape awkward; solvent is included in a small proportion of the crystals and the crystal packing in these compounds is evidently efficient. Some principles for elaboration of these systems and the design of molecular crystal lattices are considered.

Keywords: crystal packing analysis · intramolecular interactions · intermolecular interactions · multiple aryl embraces · polymorphism · structure elucidation

Introduction

Molecules with phenyl, aryl or heteroaryl groups on their surfaces frequently make use of the offset-face-to-face (OFF) and edge-to-face (EF) local pairing as part of more elaborate intermolecular molecular recognition patterns.[1] Where there are clusters of aryl groups on the surfaces of molecules a number of individual OFF and EF intermolecular aryl···aryl interactions can operate in concert, and are frequently observed to do so in crystals.[2–11] These supramolecular motifs are named as multiple phenyl (aryl) embraces because they are multi-armed, concerted, and attractive. In the case of six phenyl groups, three from each molecule, the sixfold phenyl embrace (6PE), composed of a concerted cycle of six EF interactions, is common.[3]

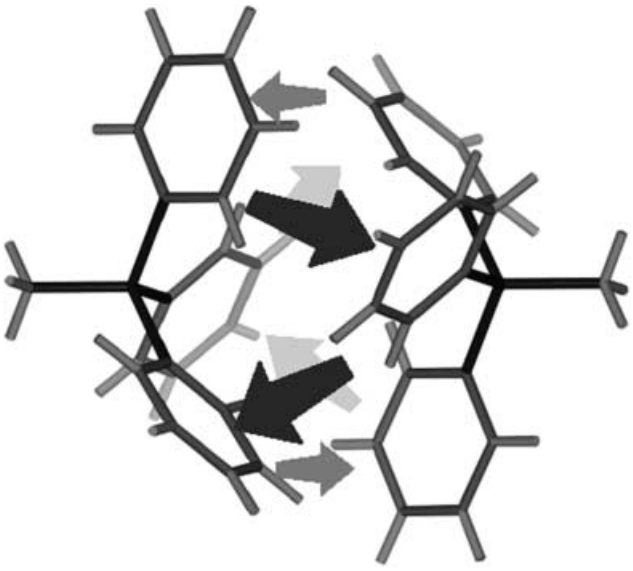

6PE

[a] Prof. I. Dance, Dr. M. Scudder
School of Chemical Sciences
University of New South Wales
Sydney, New South Wales 2052 (Australia)
Fax: (+61) 2-9385-6141
E-mail: i.dance@unsw.edu.au

0947-6539/02/0823-5456 $ 20.00+.50/0 *Chem. Eur. J.* **2002**, *8*, No. 23

Two types of compounds that engage in multiple phenyl embraces are metal complexes with PPh_3 ligands,[5–7, 9, 10, 12] and numerous anions crystallised with Ph_4P^+.[2] Metal complexes of the heteroaromatic ligands bipy, phen and terpy, and analogues, also frequently engage in embrace motifs in crystals.[11, 13] All of these systems have the phenyl or aryl groups in somewhat restricted conformations relative to the core of the molecule. There is some variability of the torsional conformations in PPh_3 metal complexes,[6] limited variability in Ph_4P^+ and its analogues, while $M(N\text{-}N)_3$ and $M(N\text{-}N\text{-}N)_2$ complexes of heteroaromatic ligands are relatively invariant in their presentation for intermolecular embraces. This conformational restriction on surface aryl groups is symbolised by **1**.

1 **2**

In this paper we consider a set of molecules characterised by additional conformational flexibility in the peripheral aryl groups, permitted by a flexible linker X, as in **2**. The molecules have the general formulation $(Ar_nX)_3Y\text{-}Z\text{-}Y(XAr_n)_3$, and have been extracted from the Cambridge Structural Database.[14] The majority of the instances have $n = 1$. There are three subsets, according to whether Z is present (**3a**), is replaced by a direct bond (**3b**) or is a void without connection between the two halves (**3c**). If Z is present it has linear geometry, and all of the systems **3** have actual, pseudo or potential threefold symmetry. There are two conformations that retain threefold symmetry and a potential centre of inversion, namely **4** (*endo*) and **5** (*exo*). We consider all relevant compounds in the CSD, none of which show conformation **6**.

$(Ar_nX)_3Y\text{-}Z\text{-}Y(XAr_n)_3$ $(Ar_nX)_3Y\text{-}Y(XAr_n)_3$ $(Ar_nX)_3Y\ \ Y(XAr_n)_3$

3a **3b** **3c**

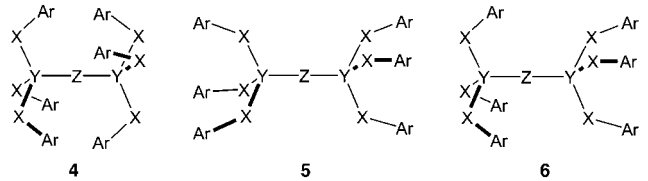

4 **5** **6**

Our analyses involve both the intra- and intermolecular interactions that are possible between Ar groups. The objective of this investigation is a refined understanding of the fundamentals of intermolecular interactions for molecules of the types considered here. This is done in the context of crystal packing: the intermolecular motifs determine the crystal packing and are revealed by analysis of it. Crystal packing is a rich source of geometrical information (although not of the crucial energy information). Since it is misleading to draw conclusions about supramolecular motifs from only part of the intermolecular domain on a molecular crystal, our analyses examine the whole intermolecular domain. The strategy of analysing the crystal packing of molecules with actual or potential symmetry is adopted to reduce the range of intermolecular motifs and, thereby, to strengthen the conclusions. Further, a general postulate of our approach is that symmetrical lattices for molecular crystals are indicative of intermolecular motifs that are more favourable and, therefore, are repeated to generate high symmetry.[10] Polymorphism,[15] or crystal packing isomerism,[16] which occurs for some of the systems discussed in this paper, is also a valuably informative phenomenon in understanding the fundamental energies of crystal packing.

In the set of compounds analyzed here there is variation of 1) the identity of Y and the Z-Y-X angle; 2) the identity and size of the central group Z, and, therefore, the Y···Y distance; 3) the presence of other groups on X; 4) substitution of the Ar groups and 5) the net charge on the molecule and the presence of counter ions or other species in the crystal.

Results and Discussion

The intramolecular sixfold phenyl embrace (6PE): We introduce the main concepts with hexabenzyldistannane $(PhCH_2)_3SnSn(CH_2Ph)_3$. This molecule adopts conformation **4**, and forms an intramolecular 6PE, illustrated in Figure 1. This 6PE has ideal symmetry in the crystal (CSD refcode SANPUS) and a relatively short distance (Sn–Sn = 2.83 Å) between the threefold centres Y. The concerted $(EF)_6$ cycle involving opposite ends of the molecule is very well developed in this molecular structure.

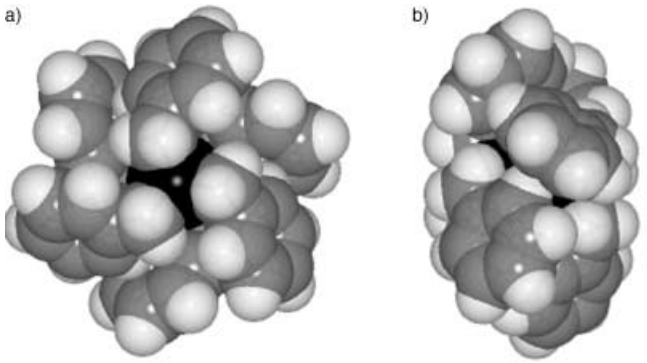

Figure 1. The intramolecular sixfold phenyl embrace (6PE) conformation of $(PhCH_2)_3SnSn(CH_2Ph)_3$ in crystals SANPUS (hydrogen atoms absent from the CSD file have been added). The molecule (with S_6 symmetry), viewed from the end (a) and side (b), possesses a well-developed cycle of six concerted edge-to-face (EF) interactions each involving phenyl groups from opposite ends of the molecule. The molecule is hexabenzyl-faceted.

The same molecular structure type occurs when there is a linear bridge Z between the Y centres, which occurs in a series of five additional molecules with linear oxide bridges between Group 4 or Group 14 metal atoms, listed in Table 1. Increase in the Y···Y separation from 2.8 to 3.8 Å has no influence on the quality of the intramolecular 6PE, because torsion at the methylene group allows adjustment, and variation of the angle of ring inclination in the EF has negligible influence on

  0947-6539/02/0823-5457 $ 20.00+.50/0

Table 1. Molecules $(PhX)_3Y\text{-}Z\text{-}Y(XPh)_3$ with an intramolecular 6PE.[a]

Compound	CSD refcode	Y···Y separation [Å]	Space group	Cell dimensions [Å], [°]
$[(PhCH_2)_3Sn]_2$	SANPUS	2.83	$R\bar{3}$	9.6, 85.8
$[(PhCH_2)_3Si]_2$-O	OXBZSI	3.23	$P\bar{1}$	9.8, 9.9, 10.3, 93.4, 115.4, 100.7
$[(2\text{-}F\text{-}C_6H_4\text{-}NH)_3Si]_2$-O	KUNGIJ	3.22	$P\bar{1}$	9.2, 9.9, 10.4, 100.6, 112.0, 92.2
$[(4\text{-}Me\text{-}C_6H_4\text{-}CH_2)_3Ge]_2$-O[b]	BZGEOX10	3.46	$R\bar{3}$	9.6 85.5
$[(PhCH_2)_3Ti]_2$-O	XBZDTI	3.61	$R\bar{3}$	9.6 83.6
$[(PhCH_2)_3Sn]_2$-O	BZSNOX01	3.82	$R\bar{3}$	9.6 84.0

[a] In this and subsequent tables, the cell parameters given for trigonal crystals are those of the rhombohedral setting, and those for triclinic structures are reduced, to facilitate comparison between analyses reported by different research groups. [b] The 4-methyl substituent has partial occupancy.

its effectiveness. Two of the compounds in Table 1 have substituted phenyl rings, as 2-fluoro ornamentation (KUNGIJ) or partial 4-methyl substitution (BZGEOX10). This also does not interfere with the intramolecular 6PE, because the substituents are directed away from or outside the interaction zone of the 6PE.[9]

Molecular aryl boxes: These molecules with six phenyl groups oriented at approximately 90° are hexafaceted and have a shape like a cubic box, with slight rhombohedral compression. As is evident in Figure 1, the principal construct of the box is the external face of the phenyl rings, the face not involved in the intramolecular $(EF)_6$ motif. For each aryl ring, one face and part edge are internal, and the other face and most of the edge are external. This edge protrudes through the box face, to create a flange on the box, as in **7**. This boxlike shape of the

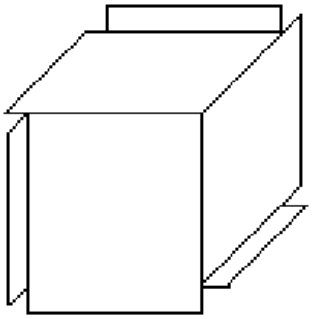

7

molecule is further illustrated in Figure 2a for $[(PhCH_2)_3Sn]_2$-O, in which the unit cell of its crystal (BZSNOX01) contains one molecule centred in the cell, and the faces of the cell parallel the faces of the box. The phenyl face and phenyl edge that comprise one face of the box are from one $(PhCH_2)_3Sn$ group, while the vertex-occupying part of that face is from the other half of the molecule.

The packing of molecular boxes: Crystalline $[(PhCH_2)_3Sn]_2$-O (and other molecules, see Table 1) has the highest lattice symmetry ($R\bar{3}$) possible for the molecular symmetry $\bar{3}$, and the cell angle is 84°. So, the crystal structure and molecular packing is easily described as a primitive packing of almost cubic molecular boxes, illustrated in Figure 2b. This packing gives rise to a number of favourable intermolecular phenyl··· phenyl interactions. Each molecule presents a phenyl face, a phenyl edge, and a phenyl vertex to its neighbour across each box face. While the vertex does not play a significant role, the edge and face are each engaged in an intermolecular EF interaction (Figure 2b), leading to an $(EF)_2$ arrangement at each box surface. In fact, considering both the intramolecular EF interactions of the 6PE and the intermolecular EF, there are continuous chains of EF interactions in the *a*, *b* and *c* directions in the crystal BZSNOX01, alternating between intra- and intermolecular in origin. The crystal packing of $[(PhCH_2)_3Sn]_2$ in SANPUS and of $[(PhCH_2)_3Ti]_2$-O in XBZDTI are essentially the same as that of $[(PhCH_2)_3Sn]_2$-O in BZSNOX01. The noninvolvement of the vertex in these interactions is relevant to the packing of the 4-phenyl-substituted molecule, $[(4\text{-}Me\text{-}C_6H_4\text{-}CH_2)_3Ge]_2$-O (BZGEOX10, Table 1), which is discussed below.

The efficiency of this crystal packing of phenyl groups—intra- and intermolecular—rivals that of crystalline benzene.

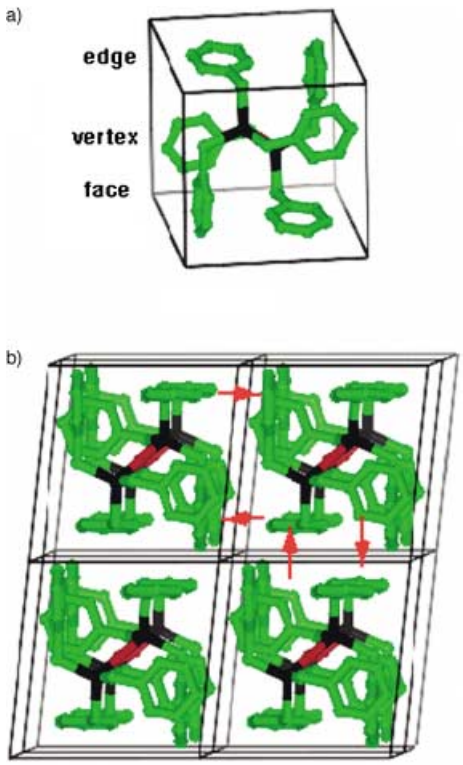

Figure 2. a) A single molecule of $[(PhCH_2)_3Sn]_2$-O (H atoms omitted) in the rhombohedral unit cell of crystals BZSNOX01 (space group $R\bar{3}$), showing how the six rings form a molecular box: the face, edge and vertex lying in the left box face are marked. b) The packing of molecular boxes of $[(PhCH_2)_3Sn]_2$-O, and the intermolecular phenyl··· phenyl interactions: the arrows indicate the locations of local edge-to-face motifs. The molecular and crystallographic threefold axis runs from the top front right vertex to the bottom back left in this figure.

0947-6539/02/0823-5458 $ 20.00+.50/0 *Chem. Eur. J.* **2002**, *8*, No. 23

Dimorphic crystal packing of phenyl boxes: Two of the compounds with intramolecular 6PE (see Table 1) crystallise in the space group $P\bar{1}$ instead of the $R\bar{3}$ lattice just described. The axial lengths of the triclinic lattice are similar to those of the rhombohedral lattice, and in both lattices there is one complete molecule per unit cell. While the molecules in the two different lattice types are different, the molecular stereochemistry, shape, size and surface features are virtually identical (see Figure 3) and, therefore, we regard this lattice duality as an instance of substitutional dimorphism.

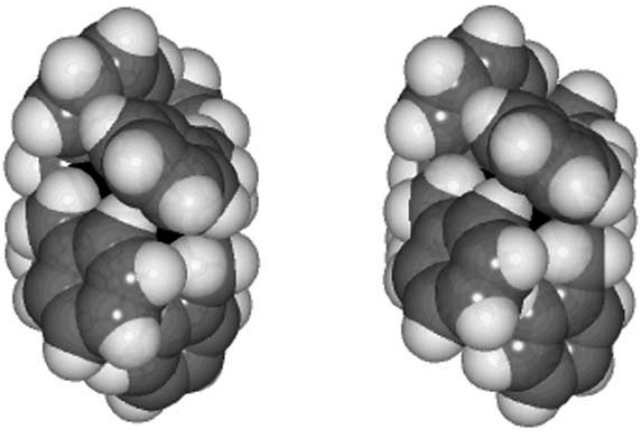

Figure 3. Comparative views of molecules $[(PhCH_2)_3Sn]_2$ and $[(PhCH_2)_3Si]_2$-O. The first molecule crystallises in the $R\bar{3}$ lattice (SANPUS), while the second crystallises in the $P\bar{1}$ lattice (OXBZSI).

Figure 4 shows aspects of the alternative triclinic crystal packing of $[(PhCH_2)_3Si]_2$ in OXBZSI. The view along *a* (Figure 4a) is similar to that of Figure 2b, and there is an intermolecular vertex-to-face (VF) interaction from the green to blue rings. However, views down the *b* and *c* axes (Figure 4b and c, respectively) show that the interactions across the box faces have been altered by slippage of the cell boxes relative to each other, with changes in the cell angles β and γ. In addition, the orientation of the molecule within the cell is such that the pseudo-threefold axis is no longer coincident with a body diagonal of the unit cell (Figure 4b, c). Concommitant with this is a notable absence of standard intermolecular phenyl $\cdots$ phenyl motifs. There are no standard phenyl $\cdots$ phenyl motifs involving the magenta or blue rings. The interactions between the blue and green rings of Figure 4 are similar to those on each face of the rhombohedral dimorph, but a slight change in the cell angle leads to involvement of the vertex, rather than the edge of the ring, so the interaction across *ac* cell faces is $(VF)_2$ instead of $(EF)_2$.

So, the difference between the rhombohedral and the triclinic packing of molecular boxes is principally that in the former there are intermolecular $(EF)_2$ interactions across all faces of the box, while in the latter there are intermolecular $(VF)_2$ interactions across only one third of the box faces. The diminished occurrence of standard motifs in the triclinic dimorph and the apparent absence of good alternative phenyl $\cdots$ phenyl interactions in two of the three directions of packing raise questions still to be answered.

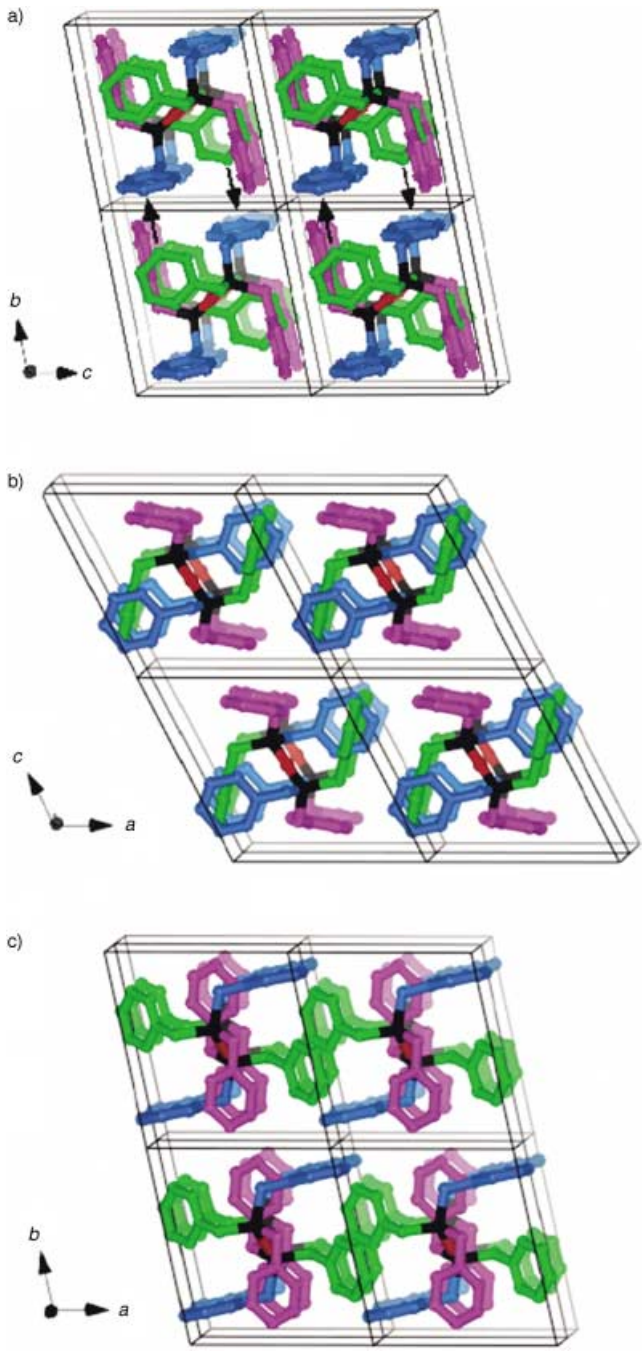

Figure 4. Three views of the crystal packing and intermolecular juxtapositions in the dimorph OXBZSI of $[(PhCH_2)_3Si]_2$-O, space group $P\bar{1}$, with one molecule centred in the unit cell. Carbon atoms of the three crystallographically different phenyl rings are coloured green, blue and magenta, and hydrogen atoms are omitted. a), b) and c) show axial representations, comparable with that in Figure 2b for the rhombohedral dimorph BZSNOX01. The projection of OXBZSI along *a* shows the occurrence of green $\rightarrow$ blue vertex-to-face (VF) local motifs (marked with arrows in a), with some similarity to those of BZSNOX01, and the cell angle α is similar in the two dimorphs. Part b) shows the sliding displacement of the packed approximately cubic molecular boxes in the *a* direction, and the concomitant increase in β to 115°. Part c) shows the projection down *c*, again different from BZSNOX01 (Figure 2b). Note from b) and c) that the pseudo threefold axis of the molecule is no longer coincident with a body diagonal of the unit cell. There are no standard phenyl $\cdots$ phenyl motifs involving the magenta rings, and nothing between blue rings. A poorly developed green HC–H $\rightarrow$ green face interaction exists. The infinite sequences of alternating intra- and intermolecular VF interactions between green (V) and blue (F) rings are evident in part b).

  0947-6539/02/0823-5459 $ 20.00+.50/0

It has already been noted that 2-fluoro- or 4-methyl-substitution of the phenyl ring does not obstruct the intramolecular 6PE. But what is the effect of phenyl substitution on the intermolecular packing? The 2-fluoro-substituted molecule $[(2\text{-F-}C_6H_4\text{-NH})_3Si]_2$-O crystallises (KUNGIJ, Table 1) in the triclinic dimorph, while the 4-methyl-substituted molecule $[(4\text{-Me-}C_6H_4\text{-}CH_2)_3Ge]_2$-O crystallises (BZGEO X10) in the rhombohedral dimorph. Full occupancy of the 4-Me substituent would lead to impossibly short $C_{Me}\cdots C_{Me}$ interactions, and the crystal reported in the CSD contains both the parent compound, $[(PhCH_2)_3Ge]_2$-O, and the substituted form, indicating that 4-substitution does not interfere with either the formation of the intramolecular 6PE or the intermolecular packing.

In passing, we comment that the 2-fluoro-substituted molecule $[(2\text{-F-}C_6H_4\text{-NH})_3Si]_2$-O is slightly different from the others in that it possesses NH–Ph rather than CH_2–Ph groups: the Si-N-C angle (129–131°) is larger than the Si-C-C angle (115–117°) of $[(Ph\text{-}CH_2)_3Si]_2$-O; this causes a flatter intramolecular 6PE with less inclined EF interactions (see Figure 5a, b). Further, the presence of H–N and C–F functions allows the possibility of intermolecular N–H···F hydrogen bonds, and one of these is present in the crystal KUNGIJ (Figure 5c). There are also good intermolecular OFF motifs in KUNGIJ (Figure 5d, e).

Ions with the intramolecular sixfold phenyl embrace: The intramolecular 6PE occurs also in molecules with positive or negative charges, specifically in $[(PhCH_2)_3P\text{-Cu-}P(CH_2Ph)_3]^+$ (three different crystals) and in $[(PhS)_3Fe\text{-O-}Fe(SPh)_3]^-$ (Table 2).

The crystal TETJAD of $[(PhCH_2)_3P\text{-Cu-}P(CH_2Ph)_3]^+$ $CuBr_2^-$ is significant because the lattice again has $R\bar{3}$ symmetry, which implies that there are efficient (and repeated) intermolecular motifs, as well as the symmetrical intramolecular 6PE. The $[(PhCH_2)_3P\text{-Cu-}P(CH_2Ph)_3]^+$ forms the same well-developed intramolecular 6PE (Figure 6a) as the

Table 2. Charged complexes possessing the intramolecular 6PE.

Compound	CSD refcode	Y···Y separation [Å]	Space group	Cell dimensions [Å], [°]
$[Et_4N]^+[(PhS)_3Fe\text{-O-}Fe(SPh)_3]^-$	FUZXED	3.53	$P2_1/a$	18.1, 15.2, 20.4, 102.5
$[(PhCH_2)_3P\text{-Cu-}P(CH_2Ph)_3]^+[CuBr_2]^-$	TETJAD	4.39	$R\bar{3}$	9.9, 88.9
$[(PhCH_2)_3P\text{-Cu-}P(CH_2Ph)_3]^+[CuCl_2]^-$	QEDHEM	4.41	$P\bar{1}$[a]	9.8 90.0
$[(PhCH_2)_3P\text{-Cu-}P(CH_2Ph)_3]^+PF_6^-$	BALMOQ	4.38	$C2/c$	14.7, 13.5, 19.5, 90.8

[a] This compound is reported as $P\bar{1}$, with lattice parameters that are exactly rhombohedral. The authors[17] could not refine the structure in the rhombohedral setting, and in the triclinic cell invoked twinning to obtain a satisfactory result.

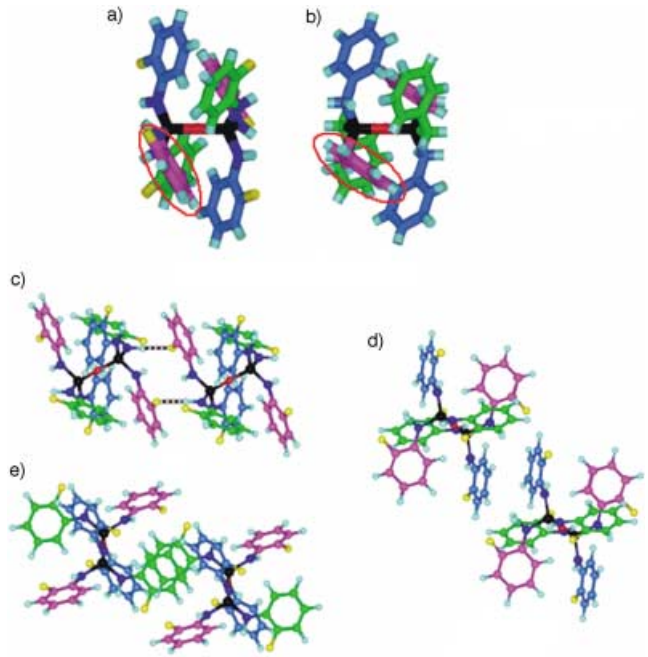

Figure 5. Aspects of the crystal structure of $[(2\text{-F-}C_6H_4\text{-NH})_3Si]_2$-O (KUNGIJ), space group $P\bar{1}$. a) The intramolecular 6PE, which is flatter than that in $[(PhCH_2)_3Si]_2$-O (OXBZSI) shown in b). The difference is highlighted by the two red ellipses. c) The intermolecular N–H···F hydrogen bond (black and white stripes, H–F = 2.05 Å) between NH of the green ligand and F of the magenta phenyl ring. d) The intermolecular OFF between green phenyl rings. e) The intermolecular OFF between blue phenyl rings.

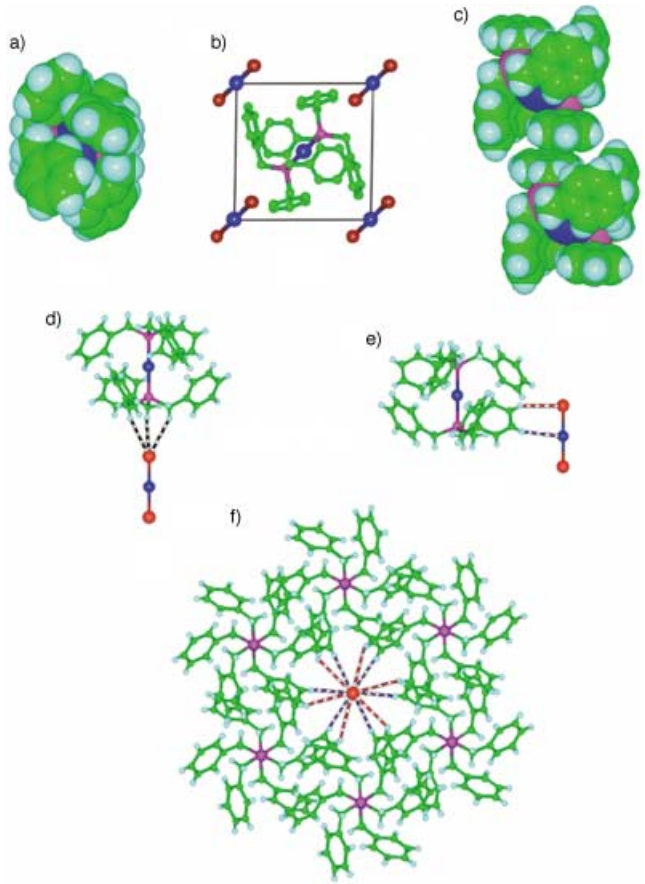

Figure 6. Relevant aspects of the crystal structure of $[(PhCH_2)_3P\text{-Cu-}P(CH_2Ph)_3]^+[CuBr_2]^-$ (TETJAD). a) The intramolecular 6PE. b) The rhombohedral unit cell (converted from the published trigonal setting), showing the location of the [Br-Cu-Br]$^-$ anions. c) Two box-shaped molecules, and the intermolecular motif **8** formed by each of its benzyl groups. d) The axial C–H···Br interactions (H···Br = 3.21 Å). e) The lateral C–H···Br (3.49 Å, red and white) and C–H···Cu (3.06 Å, blue and white) interactions. f) Threefold view of the six cations linked by C–H···Br and C–H···Cu to each anion.

0947-6539/02/0823-5460 $ 20.00+.50/0 *Chem. Eur. J.* **2002**, *8*, No. 23

neutral species described above. The rhombohedral unit cell is shown in Figure 6b and should be compared with that given in Figure 2b. The inclusion of the counter ions at the corners of the unit cells has been accompanied by a rotation of $[(PhCH_2)_3P\text{-}Cu\text{-}P(CH_2Ph)_3]^+$ within the cell, eliminating the $(EF)_2$ interactions between box faces. In their place, there is an interaction (**8**) between pairs of $PhCH_2$; this is a variant of the conventional OFF. The planar system includes the CH_2 group and the overlap is principally between the methylene H and the phenyl face. Inspection of the CSD for other occurrences of this extended OFF motif **8** indicates that it is not rare and that the CH_2 group can be methylene, or part of methyl. There is a complete network of intermolecular motifs **8** that involve the external faces of each cation, similar to the box packing described above for uncharged molecules. Figure 6c illustrates the box-shape of $[(PhCH_2)_3P\text{-}Cu\text{-}P(CH_2Ph)_3]^+$ and one of the six motifs **8** that it forms. The lattice of TETJAD accommodates the $[Br\text{-}Cu\text{-}Br]^-$ anions within this network, through C–H···Br hydrogen bonds along the threefold axis (Figure 6d) and C–H···Br and C–H···Cu hydrogen bonds laterally (Figure 6e, f).

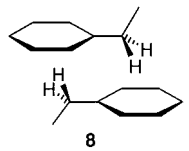

8

The crystal $[(PhCH_2)_3P\text{-}Cu\text{-}P(CH_2Ph)_3]^+PF_6^-$ (BALMOQ) forms in the monoclinic space group *C*2/*c*. In both the rhombohedral and triclinic lattices described above, the threefold axes of all molecules in the crystal are parallel. The glide plane in *C*2/*c* can and does introduce nonparallel molecular axes. However, the crystal packing in BALMOQ (Figure 7) is still similar to that described above. In the original publication of this structure,[18] the formation of the 6PE was noted, and was considered to be one of the driving forces in the molecular structure. As discussed by these authors, there is considerable hydrogen bonding within the structure of the type P–F···H. The interactions between the molecular boxes in this crystal can be described broadly as type **8** motifs in two directions, and a modification of **8** in the third, where one $Ph\text{–}CH_2$ moiety is rotated by about 90° within its plane.

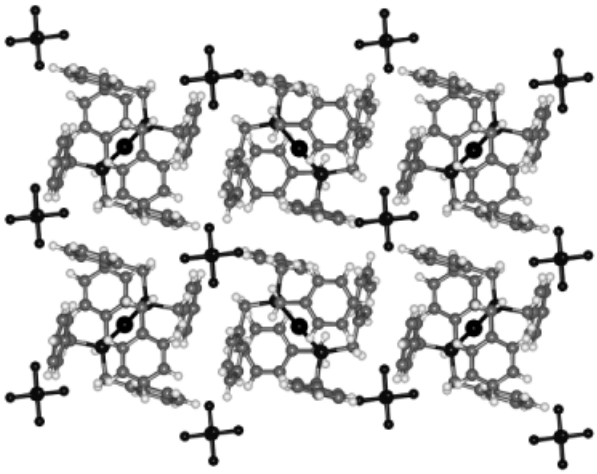

Figure 7. The crystal packing of $[(PhCH_2)_3P\text{-}Cu\text{-}P(CH_2Ph)_3]^+ PF_6^-$ (BALMOQ) viewed along the $\bar{1}10$ direction of the *C*2/*c* cell: the octahedral PF_6^- are shaded dark, Cu black, P dark. Note the packing of the molecular boxes and that the P-Cu-P axes are no longer parallel. The interactions between box faces are type **8** motifs.

Molecules in which Z vanishes: There is a series of compounds of the type $(PhX)_3Y$, in which X = S or Se and Y = As or P, that crystallise with a rhombohedral lattice in space group $R\bar{3}$, which is virtually identical to that described above in Table 1, even though there is no bond between the two Y atoms. These are listed in Table 3 and Figure 8 shows a view of a pair of molecules of $(PhS)_3As$, CATJOW, within their rhombohedral unit cell.

Table 3. Molecules $(PhX)_3Y$ which crystallise with an intermolecular 6PE to form hexafaceted dimer boxes.

Compound	CSD refcode	Y – Y separation [Å]	Space group	Cell dimensions [Å], [°]
$(PhS)_3As$	CATJOW	3.96	$R\bar{3}$	9.7, 82.3
$(PhSe)_3As$	NINRAD[a]	3.74	$R\bar{3}$	9.8, 82.5
$(PhS)_3P$	SEJRUU02	4.10	$R\bar{3}$	9.6, 82.0
$(PhSe)_3P$	VUBYUM	3.93	$R\bar{3}$	9.8, 82.1

[a] The space group in the CSD is given as *R*3, but model building suggests that the correct space group is $R\bar{3}$.

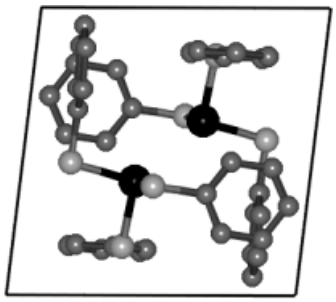

Figure 8. The rhombohedral unit cell of $(PhS)_3As$ (CATJOW) (with the origin shifted to facilitate comparison): As black, S light grey. There is no bond linking the As atoms, but the packing is very similar to that in Figure 2b for $[(PhCH_2)_3Sn]_2\text{-}O$ (BZSNOX01) with intermolecular $(EF)_2$ across each of the box faces.

Molecules with the isomeric *exo* conformation 5: The molecule $[(2\text{-}Me\text{-}PhCH_2)_3Sn]_2\text{-}O$ in crystals SANNEA has the exo molecular conformation **5** despite the fact that, as shown above, 2-substitution is no bar to formation of the *endo* conformation. It is different from its unsubstituted parent $[(PhCH_2)_3Sn]_2\text{-}O$ in crystals BZSNOX01, described above. The intramolecular characteristic of this conformation (see Figure 9a) is the presence of $(EF)_3$ motifs at each end, and the absence of an embrace between the two ends of the molecule. The molecule has the shape of tractor wheels on a single axle.

Why does this difference occur between $[(2\text{-}Me\text{-}PhCH_2)_3\text{-}Sn]_2\text{-}O$ and $[(PhCH_2)_3Sn]_2\text{-}O$? Is it due to the intramolecular or intermolecular motifs, or is **4** ⇌ **5** isomerism possible for $[(2\text{-}Me\text{-}PhCH_2)_3Sn]_2\text{-}O$ and could a dimorph containing **4** be possible? The Sn – Sn distances in SANNEA and BZSNOX01

  0947-6539/02/0823-5461 $ 20.00+.50/0

are virtually identical (3.79, 3.82 Å). The alternative isomer (**4**) for $[(2\text{-Me-PhCH}_2)_3\text{Sn}]_2\text{-O}$ has been modelled, and is shown in Figure 9b for comparison with the isomer already observed. The methyl⋯methylene juxtaposition is a little tighter in **4**, but is not considered to be strongly destabilising, and so intramolecular factors are not regarded as responsible for the difference.

Table 4. Related symmetrical molecules with the $(EF)_3$ motif at each end.

Compound	CSD refcode	Y⋯Y separation [Å]	Space group	Cell dimensions [Å], [°]
$[(2\text{-Me-PhCH}_2)_3\text{Sn}]_2\text{-O}$	SANNEA	3.79	$P\bar{1}$	10.0, 10.3, 10.8, 89.6, 72.5, 85.9
$[(\text{PhS})_3\text{C}]_2$	HPHTET	1.56, 1.59	$P\bar{1}$	9.6, 12.3, 14.8, 86.5, 80.0, 83.7
$[\{(\text{PhCH}_2)_3\text{Mo}\}_2]$	GEPKIV	2.18	$R\bar{3}$	9.5, 100.5
$[\{(\text{PhCH}_2)_3\text{W}\}_2]$	WOFMAF	2.25	$R\bar{3}$	9.6, 100.3
$[\{(2,6\text{-Me}_2\text{-PhO})_3\text{W}\}_2]$	MAPYAD	2.31	$P2_1/n$	11.8, 9.9, 18.2, 90.9
$[\{(2,4,6\text{-Me}_3\text{-PhS})_3\text{Mo}\}_2]$ + hexane[a]	CANDEA01[a]	2.23	$R\bar{3}$	11.3, 85.8
$[\{(2,4,6\text{-Me}_3\text{-PhS})_3\text{W}\}_2]$	GEKHAF	2.31	$P\bar{1}$	11.0, 11.6, 11.7, 117.4, 94.7, 97.0
$[\{(2,4,6\text{-Me}_3\text{-PhSe})_3\text{Mo}\}_2]$	VERKOS	2.22	$P\bar{1}$	11.1, 11.7, 11.7, 118.2, 96.1, 95.5
$[\{(2,4,6\text{-Me}_3\text{-PhSe})_3\text{W}\}_2]$	VERKUY	2.30	$P\bar{1}$	11.2, 11.7, 11.8, 118.3, 95.7, 95.9
$[\{\{3,5\text{-Me}_2\text{-Ph}([D_6]i\text{Pr})\text{N}\}_3\text{Mo}\}_2\text{-N}]$	VEQGON	3.64	$P\bar{1}$	10.9, 11.7, 13.4, 91.9, 102.4, 105.0
$[\{(\text{Ph}(t\text{Bu})\text{N})_3\text{Mo}\}_2\text{-P}]$	TIQMAH	4.47	$P2_1/c$	15.5, 10.5, 19.1, 103.2

[a] This lattice contains disordered hexane.[19]

The conformation **5** occurs in a number of other molecules, listed in Table 4, each with $(EF)_3$ motifs at each end. Note that the Y⋯Y separations in these molecules are generally short, down to 1.56 Å, enforcing the *exo* conformation **5**. Included in this set are four molecules with 2,4,6-methyl-substituted phenyl moieties: the methyl groups are able to participate in the EF motifs, as will be illustrated. This group of crystals exhibits the occurrence of the same two space groups as before, $P\bar{1}$ and $R\bar{3}$, presaging similar dimorphism resulting from homologation of internal atoms. The high symmetry lattice in $R\bar{3}$ is expected to have repetition of an effective intermolecular motif, which needs to be identified, but there is then a question about the reason for the lower symmetry packing of $[\{(2,4,6\text{-Me}_3\text{-PhS})_3\text{W}\}_2]$ in GEKHAF.

We start with description of the unsubstituted molecule $[\{(\text{PhCH}_2)_3\text{Mo}\}_2]$ with high symmetry packing in space group $R\bar{3}$, crystals GEPKIV (Figure 10a). $[\{(\text{PhCH}_2)_3\text{W}\}_2]$ in crystals WOFMAF is isostructural. The molecules have the tractor wheel shape (Figure 9a), with the CH_2Ph planes parallel to the molecular threefold axis and forming tight $(EF)_3$ motifs at each end. In the lattice the molecules occur along parallel threefold axes (Figure 10a), and between these axes the lattice is stabilised entirely by intermolecular benzyl⋯benzyl OFF motifs of type **8** (Figure 10a, b). The intermolecular interactions along each threefold axis (Figure 10c) involve an interleaving of the edges of phenyl groups.

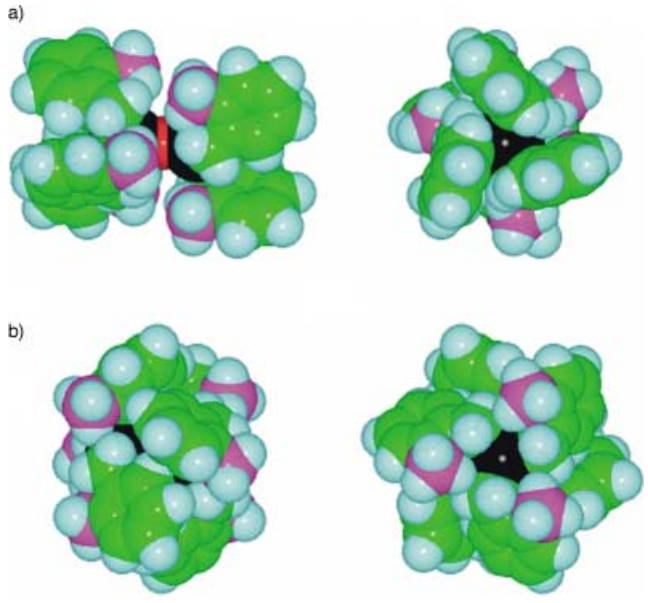

Figure 9. a) The linear centrosymmetric molecule $(2\text{-Me-PhCH}_2)_3\text{Sn-O-Sn}(\text{CH}_2\text{Ph-2-Me})_3$ as it occurs in crystals SANNEA: the C atoms of the methyl groups are coloured magenta. At each end there is a concerted $(EF)_3$ motif, and the methyl groups are concentrated in the centre. b) Comparative views of the modelled alternative isomer for the same molecule, with an intramolecular 6PE and the methyl groups (magenta) at the ends.

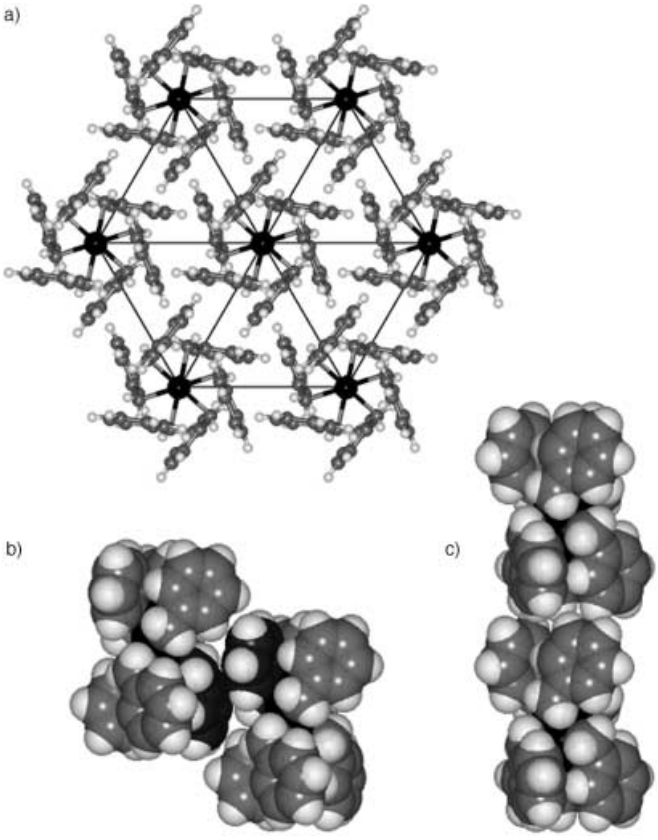

Figure 10. The crystal packing of $[\{(\text{PhCH}_2)_3\text{Mo}\}_2]$ with point group symmetry S_6 ($\bar{3}$) in crystals GEPKIV, space group $R\bar{3}$. a) Projection of the array of molecules aligned along threefold axes: the planes of the CH_2Ph groups are also parallel to the molecular threefold axes. There is only one type of lateral intermolecular motif, a type **8** OFF illustrated in b) between CH_2Ph groups with dark shading. Along the threefold axes, molecules abut as shown in the centre of c), with Ph rings fitting end to end between each other.

0947-6539/02/0823-5462 $ 20.00+.50/0 *Chem. Eur. J.* **2002**, *8*, No. 23

The centrosymmetric molecule $(PhS)_3CC(SPh)_3$ is compact, with a tight octahedron of S atoms, and two molecules in the cell of crystals HPHTET, packed primarily with a number of intermolecular EF motifs, without pseudo-packing symmetry.

Dimporphism in the four compounds [{(2,4,6-Me_3-PhQ)$_3$M}$_2$], Q = S, Se; M = Mo, W: The molecule [(2,4,6-Me_3-PhS)$_3$Mo-Mo(SPh-2,4,6-Me_3)$_3$] has S_6 symmetry, and the structure is shown in Figure 11a. The three rings at the end of each molecule still form a triangular $(EF)_3$ motif, slightly splayed open to accommodate one of the *o*-methyl substituents; this is the edge that abuts the face of the neighbouring ring (see Figure 11a). This methyl-to-phenyl face motif (well established in other systems) has alkyl–H-to-phenyl faces analogous to the well-known aryl–H-to-phenyl face. While one *o*-methyl substituent of each ligand in this molecule participates in this way in intramolecular interactions, the other *o*-methyl substituent is involved in the intermolecular motifs. The high symmetry ($R\bar{3}$) of the crystals (CANDEA01, Figure 11b) that contain this molecule leads to the occurrence of a single intermolecular motif (Figure 11c), which is a variant of motif **8** in which a methyl group, not a methylene group, is located over the adjacent phenyl face.

The molecule [(2,4,6-Me_3-PhS)$_3$W-W(SPh-2,4,6-Me_3)$_3$] is virtually identical to [(2,4,6-Me_3-PhS)$_3$Mo-Mo(SPh-2,4,6-Me_3)$_3$] just described (the metal–metal distances differ by 0.08 Å, Table 3), and yet it has different crystal packing (in GEKHAF) in space group $P\bar{1}$, and so manifests crystal packing isomerism. Most aspects of the two crystal lattices are very similar—each end of the molecule forms three lateral motifs, building layers of motifs. However, the two ends of any one molecule are engaged in adjacent layers as the molecules protrude alternately from each side of the layer. The essential difference is the constitution of the three intermolecular motifs that each end of each molecules makes with the surrounding molecules within its layer. The interactions that each $(Ar)_3$ unit makes in GEKHAF are two of type **8** and one $(EF)_2$ (Figure 12a), while those in CANDEA01 (Figure 12b) are all type **8**. This is a subtle geometrical change, and presumably corresponds to a subtle energy difference. The other difference between GEKHAF and CANDEA01 is the presence of disordered hexane solvent in the latter, causing additional separation of molecules along the threefold axis. For both crystals, the construction of the layer is such that the Y atoms are located near the surfaces.

Two other chemically homologous molecules, [{(2,4,6-Me_3-PhSe)$_3$Mo}$_2$] and [{(2,4,6-Me_3-PhSe)$_3$W}$_2$], adopt the same triclinic crystal structure as GEKHAF (see Table 4). In an attempt to rationalise the dimorphism in the set of four compounds [{(2,4,6-Me_3-PhQ)$_3$M}$_2$] (Q = S, Se; M = Mo, W), we note that the higher symmetry structure type (Figure 12b) is formed by the smallest molecule and this higher symmetry dimorph, which incorporates poorly packed alkane solvent, appears to be the less stable.

Experimentally the dimorphism is subtle, because [{(2,4,6-Me_3-PhS)$_3$Mo}$_2$] and [{(2,4,6-Me_3-PhS)$_3$W}$_2$] crystallised from the same solvent mixture.[19] We postulate that the alternate crystal packing type for each could be generated by different crystallisation conditions.

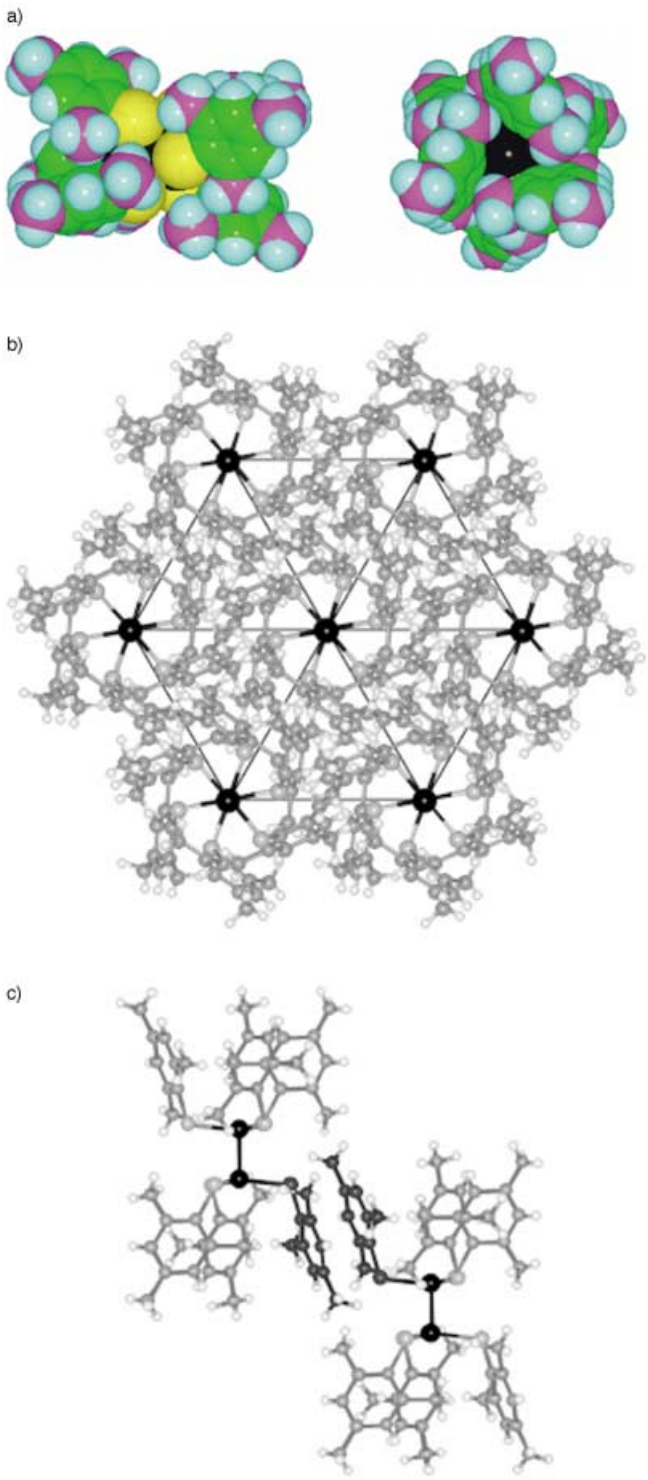

Figure 11. Aspects of the molecular structure of [{(2,4,6-Me_3-PhS)$_3$Mo}$_2$] in crystals CANDEA01. a) The molecule, symmetry S_6, with the methyl carbon atoms coloured magenta, to show how the intramolecular triangular $(EF)_3$ motif uses *o*-methyl hydrogen atoms rather than phenyl hydrogen atoms as the edge. b) Three-fold view of the $R\bar{3}$ lattice. c) The motif **8**, (dark shading) with a plane separation of 3.5 Å, that links all molecules in the lattice. There is considerable space between molecules translated along the threefold axis, occupied by disordered hexane.

Again there are compounds in which the Z linker is absent, and in which there is no Y–Y bond, that are analogous to those described in this section. There are two dimorphs of

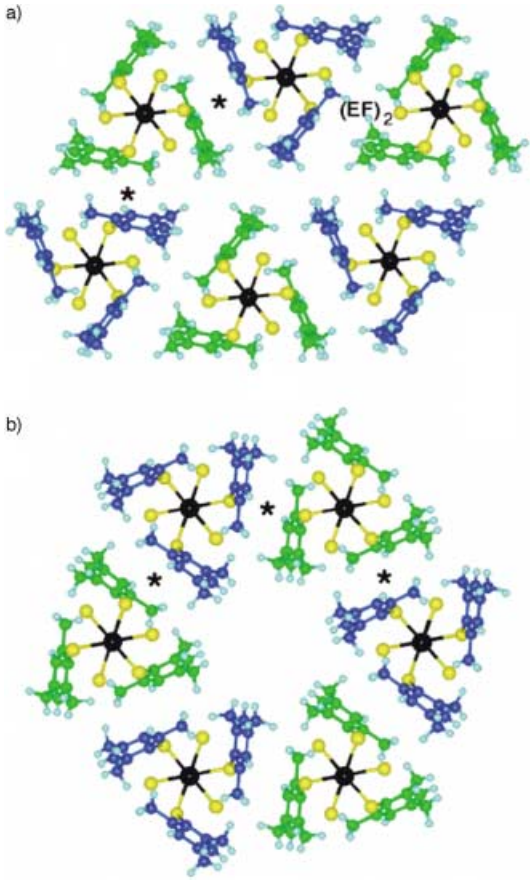

Figure 12. Comparison of the lateral intermolecular motifs in GEKHAF ([{(2,4,6-Me_3-PhS)$_3$W}$_2$]) and CANDEA01 ([{(2,4,6-Me_3-PhS)$_3$Mo}$_2$]). In each case rings other than those in a layer are omitted (i.e., only half of each molecule is shown) and the alternation of direction of the "cup" of the $(EF)_3$ motif is distinguished by colour (green points down, blue points up). a) Part of the layer of molecules in GEKHAF, in which the intermolecular motifs are two type **8** motifs (represented by *) and one $(EF)_2$. This is a subtle variation of the three type **8** interactions engaged by each end of the molecule in CANDEA01, shown in b). The space in the centre of the layer in b) is occupied by the disordered hexane solvent.

[(Ph-CH(CH_3))$_3$N], GUBPUO and GUBQAV, in space groups $R\bar{3}$ and $P2_12_12_1$, respectively. The molecular conformation in both forms has the $(EF)_3$ cycle of phenyl rings (Figure 13a). The rhombohedral variant has two crystallographically distinct molecules, each with threefold symmetry. The crystal packing is made up of two different, but similar layers, each composed of only one of the two distinct molecules. The layer is similar to that for CANDEA01 (Figure 12b), but the orientation of the molecules within the layer is such that the interface between adjacent molecules is a pair of composite edge-to-face and methyl-to-face (MF) interactions (Figure 13b) rather than the extended OFF motif (**8**). The N atoms in each of these layers are coplanar and located at the centre of the layers. As for CANDEA01, the orientations of the intramolecular $(EF)_3$ cups alternate up and down as shown in Figure 13c. There are no layers in the orthorhombic polymorph.

Compounds with PhNR ligands: The related molecules **9** and **10** also form (well-developed) $(EF)_3$ motifs at either end, shown in Figure 14. The alkylamide substituents are concen-

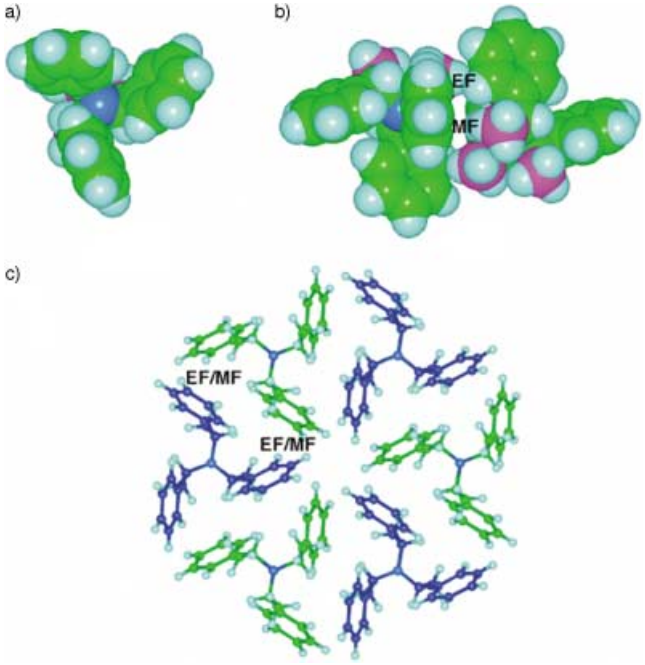

Figure 13. a) A molecule of (Ph-CH(CH_3))$_3$N in the rhombohedral dimorph, GUBPUO, showing the $(EF)_3$ conformation of the three phenyl rings. b) The intermolecular motif propagated throughout the structure, where one phenyl face takes part in both an edge-to-face (EF) and methyl-to-face (MF) interaction. c) A layer of molecules in GUBPUO, to be compared with that found in CANDEA01 (Figure 12b). Molecules with their $(EF)_3$ cups directed upward are blue, while those that point downward are green.

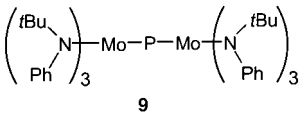

9

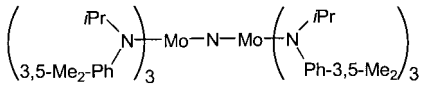

10

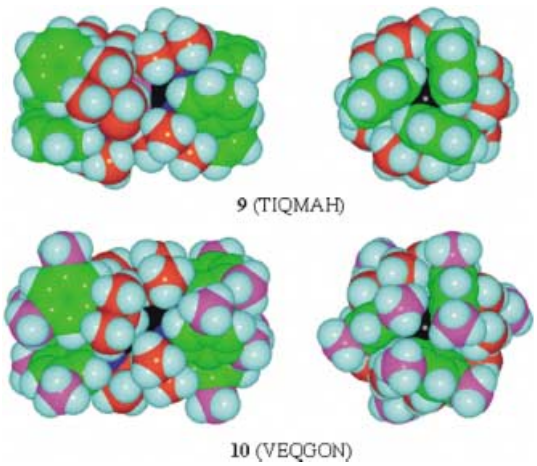

Figure 14. The molecular structures **9** (TIQMAH) and **10** (VEQGON), showing the retention of the end $(EF)_3$ motifs. The C atoms of amide alkyl groups are coloured orange, and those of the ring methyl groups in **10** are coloured magenta.

0947-6539/02/0823-5464 $ 20.00+.50/0 *Chem. Eur. J.* **2002**, *8*, No. 23

trated in the central domain of the molecule, and the methyl substituents at the 3,5-positions on the phenyl ring in **10** are out of the EF domain. Molecule **10** is an unusual example of a molecule that is largely coated with alkyl groups and yet is conformationally maintained by aryl ··· aryl motifs.

The alkylation of these molecules naturally diminishes the occurrence of intermolecular aryl motifs. In crystalline **9** (TIQMAH) the molecules are aligned coaxially (see Figure 15) as is characteristic of most of the crystal structures described above, but there are only a few EF motifs between molecules.

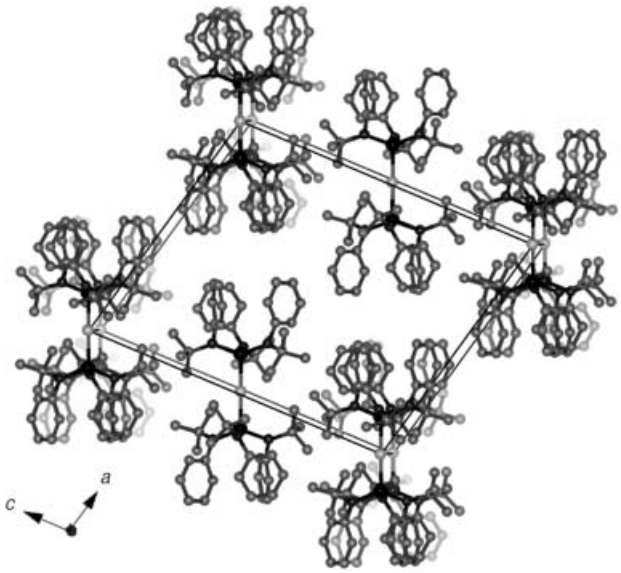

Figure 15. The coaxial array of molecules **9** in TIQMAH, with H atoms omitted. There are some intermolecular EF motifs in the *ab* plane, at $c = 0$.

$[(Ph_2N)_3Ti\text{-}O\text{-}Ti(NPh_2)_3]$—a combination of intramolecular 6PE and $(EF)_3$ motifs: If both amide substituents are phenyl, the possibility exists for one set of phenyl rings to form an intramolecular 6PE and the other set the $(EF)_3$ motifs. This combination occurs in $[(Ph_2N)_3Ti\text{-}O\text{-}Ti(NPh_2)_3]$, crystals GENQEV. This totally phenylated molecule is illustrated in Figure 16a, and both types of intramolecular embrace, $(EF)_6$ in the centre and $(EF)_3$ at each end, are well developed. The combination of these intramolecular motifs changes the shape of the molecule, such that the favourable intermolecular motifs characteristic of the separate intramolecular features are thwarted by mutual interference. The faces of the central box region are partly covered by the tractor wheels and are unable to form EF or OFF with neighbours; the central faces also enlarge the axle between the tractors wheels, blocking the interactions formed by less elaborate molecules. Consequently the crystal packing does not show good intermolecular phenyl ··· phenyl motifs (see Figure 16b).

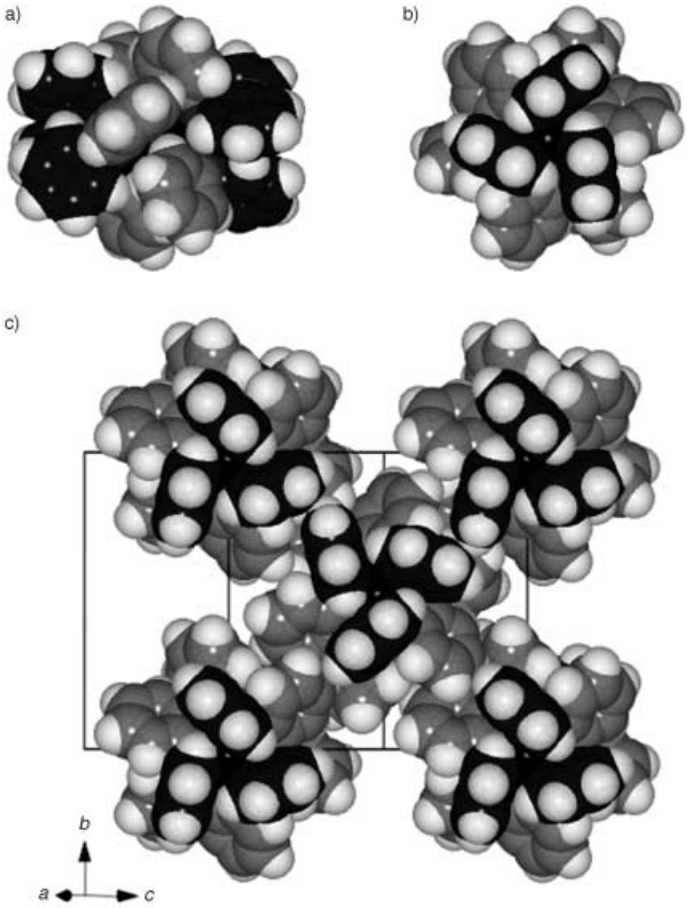

Figure 16. a) The molecule $[(Ph_2N)_3Ti\text{-}O\text{-}Ti(NPh_2)_3]$, in which one set of phenyl rings (light shading) forms the central intramolecular 6PE, and the other set (dark shading) forms the $(EF)_3$ motifs at either end of the molecule. b) Part of the crystal packing, in GENQEV (space group $P2_1/c$). The threefold molecules are approximately coaxial, and those in the layer shown are arranged rectangularly, and intermolecular phenyl ··· phenyl motifs are poorly developed.

Molecules $[(Ph_3X)_3Y\text{-}Z\text{-}Y(XPh_3)_3]$: Finally we describe some molecules with three phenyl groups on each of the three ligands on Y (the metal). They are listed in Table 5. Four of the crystals contain the $[(Ph_3X)_3Ag\text{-}CN\text{-}Ag(XPh_3)_3]^+$ complex

Table 5. Crystals containing species of type $(Ph_3X)_3Y\text{-}Z\text{-}Y(XPh_3)_3$. The space group is $P\bar{1}$ in each case.

Compound	CSD refcode	Triclinic cell dimensions [Å], [°]	Intramolecular motifs
$[\{(Ph_3P)_3Ag\}_2\text{-}(CN)]^+$ $[NCAgCN]^- \cdot (pyridine)_3$	PAWFIC	13.5, 14.3, 15.3, 85.7, 85.6, 69.3	$(EF)_{12}$, $[(EF)_3]_2$
$[\{(Ph_3As)_3Ag\}_2\text{-}(CN)]^+$ $[NCAgCN]^- \cdot (pyridine)_3$	PAWFOI	13.7, 14.4, 15.5, 85.8, 86.1, 68.8	$(EF)_{12}$, $[(EF)_3]_2$
$[\{(Ph_3P)_3Ag\}_2\text{-}(CN)]^+$ $[NCAgCN]^- \cdot (2\text{-picoline})_2 \cdot H_2O$	PAWFUO	14.5, 14.7, 25.8, 79.8, 85.0, 85.5	$(EF)_{12}$, $[(EF)_3]_2$
$[\{(Ph_3P)_3Ag\}_2\text{-}(CN)]^+$ $[NCAgCN]^- \cdot (MeCN)_2$	PAWGAV	13.6, 13.9, 16.7, 98.9, 110.0, 113.0	$(EF)_{12}$, $[(EF)_3]_2$
$[\{(Ph_3P)_3Cu\}_2\text{-}(CN)]^+$ $[(NC)_2C{=}C(CN)_2]^-$	YAZPIY	13.0, 14.4, 14.6, 106.4, 116.2, 90.6	$(OFF)_6(EF)_6$, $[(EF)_3]_2$

  0947-6539/02/0823-5465 $ 20.00+.50/0

(X = P or As) with $[NCAgCN]^-$ and various solvents, although they are not isomorphous. A key feature of the molecular structure (with pseudo-S_6 symmetry) is the presence of twelve phenyl rings in a cycle of EF interactions around the equator of the molecule, while the standard $(EF)_3$ motif occurs at each end of the molecule. These impressive intramolecular embraces are illustrated in the side and end views of the molecule in Figure 17a. The 12 EF motifs in the central set are concerted, as shown diagrammatically in Figure 17b, and alternate between Ph_3P ligands on the same and opposite ends of the molecule. This $(EF)_{12}$ pattern is analogous to the 12 PE which we have previously described[5] when two molecules of $[Pd(PPh_3)_3]$ are paired in crystals VACKEP. The phenyl-based *inter*molecular motifs for the compounds listed in Table 5 are less well developed, as is evident simply from the variable composition of the additional components of four crystals PAWFIC, PAWFOI, PAWFUO and PAWGAV (Table 5). Part of the crystal packing of PAWFIC is shown in Figure 17c.

In passing at this point, we draw attention to the existence of a chemically different metal complex, $[(Ph_2AsCH_2CH_2)_3N\text{-}Ni\text{-}I\text{-}Ni\text{-}N(CH_2CH_2AsPh_2)_3]^+$ (Figure 18), which is approximately spherical and also possesses an intramolecular concerted cycle of twelve phenyl rings.

The one copper complex in Table 5, $[(Ph_3P)_3Cu\text{-}CN\text{-}Cu(PPh_3)_3]^+$ crystallised with $[(NC)_2C{=}C(CN)_2]^-$ in YAZPIY, has a different intramolecular conformation, shown in Figure 19. While the standard $(EF)_3$ motifs are retained at the ends of the molecule, the central region involves a rich interplay of EF and OFF motifs, such that each phenyl ring is involved in four motifs.

Conclusion

We have drawn attention to a number of patterns of intra- and intermolecular geometry in molecular crystals already recorded in the literature. These patterns are based on phenyl···phenyl (including substituted phenyl) interactions, which are concerts of the basic EF and OFF motifs. The molecules are dominated by intramolecular multiple phenyl embraces, and the crystal packing is dominated by repeated phenyl···phenyl motifs. A result of this repetition of evidently favourable motifs is high crystal symmetry, or, where crystal symmetry is low, a relatively small variety of intermolecular motifs.

To recapitulate the patterns…

1. Molecules $(Ph'X)_3Y\text{-}Z\text{-}Y(XPh')_3$ (Ph′ is Ph or substituted Ph) can form an intramolecular 6PE, with concerted $(EF)_6$, which folds the molecule into a rhombohedral box with exact or approximate S_6 symmetry. They have the *endo* conformation **4**.
2. Crystals of these molecules with intramolecular 6PE are formed by three-dimensional stacking of the rhombohedral boxes. The intermolecular phenyl···phenyl motifs occur with two possibilities, evident as dimorphic crystals. One lattice has a simple stacking of the molecular boxes, yielding crystals in space group $R\bar{3}$, while the second lattice has the molecular boxes displaced relative to each other

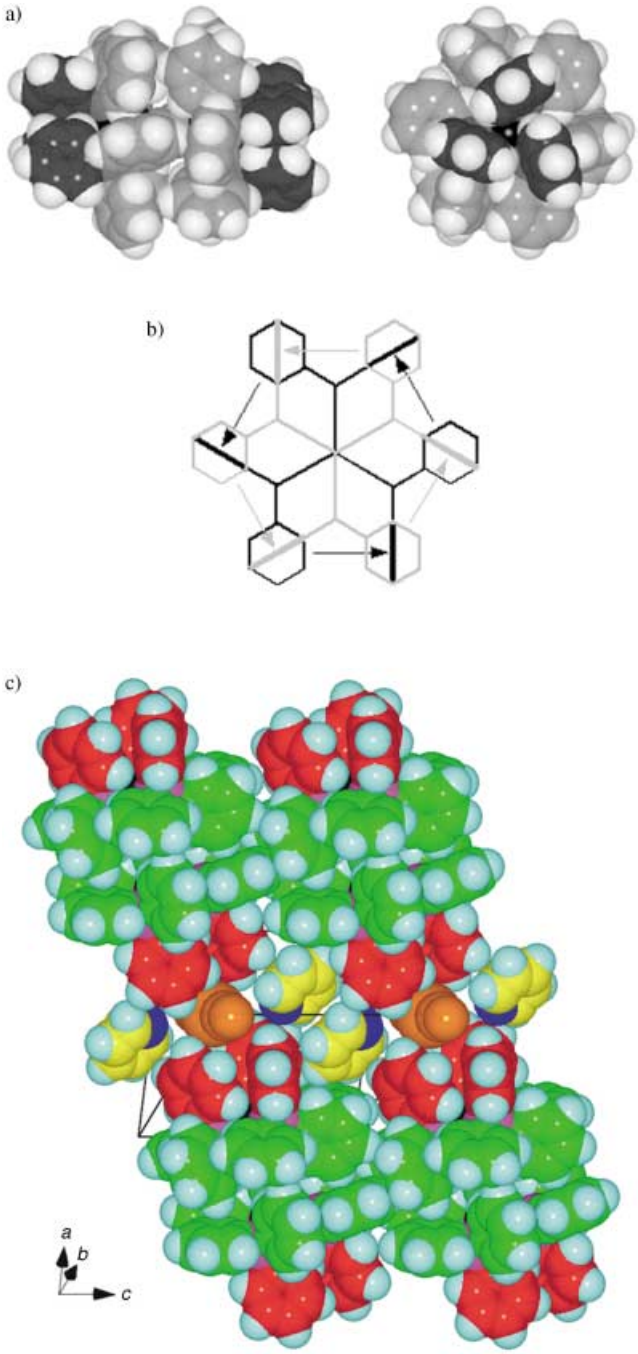

Figure 17. a) The molecular structure of $[(Ph_3P)_3Ag\text{-}CN\text{-}Ag(PPh_3)_3]^+$, showing the $(EF)_3$ motif at each end of the molecule (C atoms with dark shading) and the concerted cycle of twelve EF motifs around the equator of the molecule (C atoms with light shading). The bridging CN is disordered and the molecule is effectively centrosymmetric. The phenyl···phenyl interactions between the two hemispheres of the molecule are actually vertex to face (VF), while those within each hemisphere are EF. b) Diagram of the concerted cycle phenyl···phenyl interactions around the centre of the molecule, with the two hemispheres coloured black and grey. The interactions between rings in the same hemisphere but different ligands are marked with edge to face arrows, while those between the hemispheres are viewed parallel to the edge and perpendicular to the face. c) Part of the crystal packing of $[\{(Ph_3P)_3Ag\}_2\text{-}(CN)]^+$ with $[NCAgCN]^-$ (coloured orange) and pyridine (yellow and blue) in crystals PAWFIC (space group $P\bar{1}$). Note that the additional components separate the molecules at the $(EF)_3$ ends (red), while there is some intermolecular gearing of the equatorial phenyl groups (green).

0947-6539/02/0823-5466 $ 20.00+.50/0 *Chem. Eur. J.* **2002**, *8*, No. 23

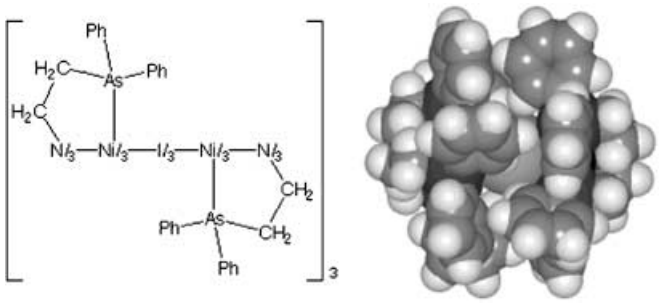

Figure 18. The complex $[(Ph_2AsCH_2CH_2)_3N\text{-}Ni\text{-}I\text{-}Ni\text{-}N(CH_2CH_2AsPh_2)_3]^+$ in crystals DPASNI10 (with tetraphenylborate and tetrahydrofuran), with the intramolecular Ph_{12} motif shown in Figure 17b. Within each hemisphere of the molecule there is a concerted cycle of six EF interactions, and between the two hemispheres there are six vertex to face (VF) interactions.

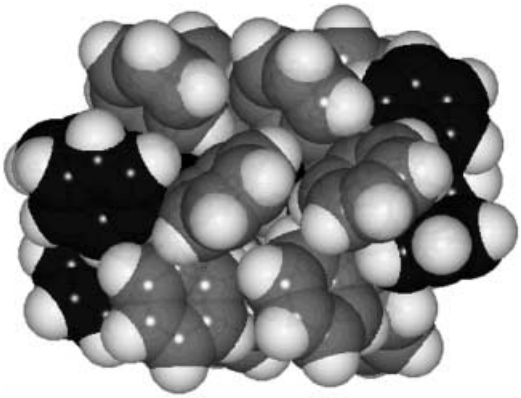

Figure 19. The intramolecular phenyl $\cdots$ phenyl motifs in $[(Ph_3P)_3Cu\text{-}CN\text{-}Cu(PPh_3)_3]^+$ (YAZPIY). The $(EF)_3$ motif occurs at each end of the molecule (darkly shaded carbon atoms), while in the central region there are $(EF)_6$ cycles within each hemisphere (i.e., Cu coordination) and approaches to $(OFF)_6$ across the equator, generating also $(EF)_6$ across the equator. Each phenyl ring in the central domain (lightly shaded carbon atoms) is involved four EF motifs and one OFF motif, although these motifs have imperfections.

mainly in one dimension, yielding crystals in space group $P\bar{1}$.

3. These intra- and intermolecular motifs permit volume-efficient packing of phenyl groups, surrounded by EF and OFF interactions within and without the molecule, and challenging the packing efficiency of benzene.
4. Charged metal complexes with suitable ligands can form the intramolecular 6PE, and, with suitable counter ions, crystallise with high symmetry.
5. Where the Y$\cdots$Y separation in $(Ph'X)_3Y\text{-}Z\text{-}Y(XPh')_3$ is relatively short the molecular conformation becomes *exo* (**5**), enabled by the formation of concerted $(EF)_3$ motifs at either end of the threefold molecule, suggesting a tractor wheel metaphor.
6. These molecules with $(EF)_3\text{–}(EF)_3$ intramolecular motifs also pack efficiently by using the external faces and edges to form intermolecular phenyl $\cdots$ phenyl motifs. Again there are dimorphic forms of this crystal packing, but both are characterised by parallel (or virtually parallel) molecular threefold axes. Again there is efficient volume packing of phenyl groups.
7. Molecules with X = NR retain the same properties, but modification of molecular shape through R is possible. When R = Ph, in $[(Ph_2N)_3Ti\text{-}O\text{-}Ti(NPh_2)_3]$, both types of intramolecular multiple phenyl embrace motif are possible, and occur as $(EF)_3 + (EF)_6 + (EF)_3$.
8. In the class $(Ph_3X)_3Y\text{-}Z\text{-}Y(XPh_3)_3$, more extensive intermolecular phenyl embraces occur. $[(Ph_3P)_3Ag\text{-}CN\text{-}Ag(PPh_3)_3]^+$ manifests $(EF)_{12}$ in the central domain and $(EF)_3$ at each end, while $[(Ph_3P)_3Cu\text{-}CN\text{-}Cu(PPh_3)_3]^+$ is $(EF)_6$ plus $(OFF)_6$ in the centre and $(EF)_3$ at each end: the difference is probably a consequence of the associated anions and crystal packing.
9. These elaborate and heavily phenylated molecules become more spherical, rather than boxlike or tractor wheel-like, and the intermolecular interactions are less able to use specific pairwise phenyl $\cdots$ phenyl motifs.
10. A single-crystal packing motif, occurring on each face of a multifaceted molecule, can be sufficient to stabilise the full crystal lattice.
11. Molecules which may be considered "half" of those described above, that is, $(ArX)_3Y$, can pack in analogous ways. They crystallise with their rings in either the *endo* (**4**) or *exo* (**5**) arrangement, and those in the *endo* form can display an intermolecular 6PE. Rhombohedral crystal symmetry can be displayed by these compounds.
12. Finally, we note the occurrence in many of the crystals described above of a modification of the offset face-to-face (OFF) motif, involving substituent methylene (or methyl) groups. Instead of the overlap being between the phenyl rings, the geometry of the interaction is such that the major overlap is between a $-CH_2$ group and a phenyl ring, as in **8**.

Some general principles are evident. The crystals described are largely devoid of solvent, which corroborates the conclusion that there is efficient crystal packing: we regard inclusion of small solvent molecules with nonhost molecules as possible indication of poor crystal packing (unless there are strong intermolecular interactions involving the solvent). Solvent inclusion in crystal lattices often occurs with shape-awkward molecules, while the molecules described here are shape-auspicious. Many of the crystals analysed in this paper are remarkable, because they use essentially only one type of supramolecular interaction.

Further, the crystals described are also devoid of strong hydrogen bonding and functional groups that can hydrogen-bond strongly. This raises the question as to whether the efficient and hydrophobic phenyl packing motifs observed have competitively excluded conventional hydrogen bonding. We are not yet able to answer this question.

Where might this lead? We refrain from discussing this molecular crystal chemistry in terms of crystal engineering, because we believe that engineering follows design, and design requires fundamental understanding of all parts of the intermolecular domain in crystals. The objective here is to advance that understanding to the extent that it can be used in design. A key component of understanding is knowledge of the relative energies of the relevant intra- and intermolecular motifs, and of alternatives. Enthusiasm for engineering is

curbed by the appearance of polymorphism, the nemesis of crystal design, in the systems described here.

Nevertheless, we have described here a set of diverse molecular types that could be elaborated synthetically in a variety of ways, some of which should not be difficult synthetically. There are ideas that could survive further testing. One is that threefold molecules frequently are arranged in crystals with parallel threefold axes,[4, 10, 20] allowing for molecular gearing like that shown in Figure 10. This also facilitates alignment of metal sites within the molecules. Another postulate is that molecules with flexible phenyl or aryl groups on their surfaces are likely to be enclosed by those phenyl groups, presenting a hydrophobic exterior able to participate further in aryl $\cdots$ aryl intramolecular motifs and affect the properties of the crystals. Another idea is to introduce strongly hydrogen-bonding functionalities on the phenyl group or at X in molecules $(Ph_nX)_3Y\text{-}Z\text{-}Y(XPh_n)_3$. A further point is the common occurrence of intra- and intermolecular inversion centres, disqualifying these molecular types for the design of chiral molecules or noncentric crystals. All of the molecules described in this paper have equivalent ends, but chiral molecules with inequivalent ends are still to be investigated experimentally.

Finally, continued investigation of the actual and nascent crystal polymorphism of these compounds, particularly variations of crystallisation conditions and procedures by those holding samples, are likely to inform the fundamental understanding of intermolecular interactions and the potential for crystal design and fabrication.

Acknowledgement

This research is supported by the Australian Research Council and the University of New South Wales.

[1] Abbreviations used, OFF offset-face-to-face, EF edge-to-face, VF vertex-to-face, MF methyl-to-face, 6PE sixfold phenyl embrace.

[2] U. Muller, P. Klingelhofer, J. Eicher, R. Bohrer, *Z. Kristallogr.* **1984**, *168*, 121 – 131; I. Dance, M. Scudder, *J. Chem. Soc. Dalton Trans.* **1996**, 3755 – 3769; I. Dance, M. Scudder, *Chem. Eur. J.* **1996**, *2*, 481 – 486; M. Scudder, I. Dance, *J. Chem. Soc. Dalton Trans.* **1998**, 3167 – 3176; M. Scudder, I. Dance, *J. Chem. Soc. Dalton Trans.* **1998**, 3155 – 3166; U. Muller, A. Noll, *Z. Anorg. Allg. Chem.* **2000**, *626*, 2438 – 2440.

[3] I. G. Dance, M. L. Scudder, *J. Chem. Soc. Chem. Commun.* **1995**, 1039 – 1040.

[4] C. Hasselgren, P. A. W. Dean, M. L. Scudder, D. C. Craig, I. G. Dance, *J. Chem. Soc. Dalton Trans.* **1997**, 2019 – 2027; M. Scudder, I. Dance, *J. Chem. Soc. Dalton Trans.* **1998**, 329 – 344.

[5] I. Dance, M. Scudder, *New J. Chem.* **1998**, *22*, 481 – 492.

[6] I. G. Dance, M. L. Scudder, *J. Chem. Soc. Dalton Trans.* **2000**, 1579 – 1586.

[7] I. G. Dance, M. L. Scudder, *J. Chem. Soc. Dalton Trans.* **2000**, 1587 – 1594.

[8] S. Lorenzo, C. Horn, D. Craig, M. L. Scudder, I. G. Dance, *Inorg. Chem.* **2000**, *39*, 401 – 405; T. Steiner, *Trans. Am. Crystallogr. Assoc.* **1998**, *33*, 165 – 173; T. Steiner, *New J. Chem.* **2000**, *24*, 137 – 142.

[9] M. L. Scudder, I. G. Dance, *J. Chem. Soc. Dalton Trans.* **2000**, 2909 – 2915.

[10] I. G. Dance, M. L. Scudder, *New J. Chem.* **2001**, *25*, 1500 – 1509; I. G. Dance, M. L. Scudder, *New J. Chem.* **2001**, *25*, 1510 – 1515.

[11] V. M. Russell, M. L. Scudder, I. G. Dance, *J. Chem. Soc. Dalton Trans.* **2001**, 789 – 799.

[12] I. G. Dance, M. L. Scudder, *CrystEngComm* **2001**, *3*, 46 – 49.

[13] I. Dance, M. Scudder, *J. Chem. Soc. Dalton Trans.* **1998**, 1341 – 1350; M. L. Scudder, H. A. Goodwin, I. G. Dance, *New J. Chem.* **1999**, *23*, 695 – 705; C. Horn, B. F. Ali, I. G. Dance, M. L. Scudder, D. C. Craig, *CrystEngComm* **2000**, *2*, 6 – 15; C. Horn, M. L. Scudder, I. G. Dance, *CrystEngComm* **2000**, *2*, 53 – 66; C. Horn, M. L. Scudder, I. G. Dance, *CrystEngComm* **2000**, *2*, 196 – 201; C. Horn, M. L. Scudder, I. G. Dance, *CrystEngComm* **2001**, *3*, 9 – 14; C. Horn, M. L. Scudder, I. G. Dance, *CrystEngComm* **2001**, *3*, 1 – 8; C. Horn, L. Berben, H. Chow, M. L. Scudder, I. G. Dance, *CrystEngComm* **2002**, *4*, 7 – 12; N. W. Alcock, P. R. Barker, J. M. Haider, M. J. Hannon, C. L. Painting, Z. Pikramenou, E. W. Plummer, K. Rissanen, P. Saarenketo, *J. Chem. Soc. Dalton Trans.* **2000**, 1447 – 1461; M. J. Hannon, C. L. Painting, E. A. Plummer, L. P. Childs, N. W. Alcock, *Chem. Eur. J.* **2002**, *8*, 2226 – 2238.

[14] F. H. Allen, O. Kennard, *Chemical Design Automation News* **1993**, *8*, 131 – 137.

[15] W. C. McCrone, in *Polymorphism in Physics and Chemistry of the Organic Solid State*, *Vol. II* (Eds.: D. Fox, M. M. Labes, A. Weissemberg), Interscience, New York **1965**, p. 726; J. Bernstein, in *Organic Solid State Chemistry* (Ed.: G. R. Desiraju), Elsevier, Amsterdam **1987**, pp. 471 – 518; J. D. Dunitz, J. Bernstein, *Acc. Chem. Res.* **1995**, *28*, 193 – 200; M. R. Caira, in *Design of Organic Solids*, *Vol. 198* (Ed.: E. Weber), Springer, Berlin **1998**, p. 163 – 208; D. Braga, F. Grepioni, *Chem. Soc. Rev.* **2000**, *29*, 229 – 238.

[16] J. D. Dunitz, in *Perspectives in Supramolecular Chemistry: The Crystal as a Supramolecular Entity*, *Vol. 2* (Ed.: G. R. Desiraju), Wiley, Cheichester **1996**, pp. 1 – 30.

[17] E. W. Ainscough, A. M. Brodie, A. K. Burrell, G. H. Freeman, G. B. Jameson, G. A. Bowmaker, J. V. Hanna, P. C. Healy, *J. Chem. Soc. Dalton Trans.* **2001**, 144 – 151.

[18] E. W. Ainscough, A. M. Brodie, A. K. Burrell, J. V. Hanna, P. C. Healy, *Inorg. Chem.* **1999**, *38*, 201 – 203.

[19] M. H. Chisholm, J. F. Corning, K. Folting, J. C. Huffman, *Polyhedron* **1985**, *4*, 383 – 390.

[20] C. Horn, I. G. Dance, D. Craig, M. L. Scudder, G. A. Bowmaker, *J. Am. Chem. Soc.* **1998**, *120*, 10549 – 10550.

Received: June 24, 2002 [F4201]

